major components of muscle tissue. Of the 425 cDNA clones, actin (2 forms) occurred 80 times (19%) and myosin (11 forms) was found 68 times (16%). The remaining ESTs could be classified as being involved in gene/protein expression (3%), immunity (7%), metabolism (31%), protein binding (7%), or cell signaling (8%) (Fig. 1). Some identified genes (11%) could not be classified into any of these groups.

The sequences of all the ESTs generated from the bay scallop cDNA library and the putative identifications determined to date are available on a Bay Scallop EST project website (http://www.mbl.edu/goetz/EST.html) as well as in NCBI's GenBank database (http://www.ncbi.nlm.nih.gov/) [GenBank Accession numbers CF197421-CF197787]. The ESTs generated offer a valuable resource to scientists in a wide range of disciplines including muscle physiology, growth and development, immunity, genetic identification, and aquaculture.

Funding for this research was provided by USDA grant #2002-03633—Program in Growth and Nutrient Utilization.

Literature Cited

1. **Garczynski, M. A., and F. W. Goetz. 1997.** *Biol. Reprod.* **57:** 856–864.
2. **Altschul, S. F., W. Gish, W. Miller, E. W. Myers, and D. J. Lipman. 1990.** *J. Mol. Biol.* **215:** 403–410.

Reference: *Biol. Bull.* **205:** 228–230. (October 2003)

Scanning Electron Microscopy Investigation of Epizootic Lobster Shell Disease in *Homarus americanus*

A. C. Hsu[1] and R. M. Smolowitz[2,]*
[1] Boston University Marine Program, Woods Hole, MA
[2] Marine Biological Laboratory, Woods Hole, MA

The American lobster, *Homarus americanus,* represents an important fishery for much of the New England coast as well as several coastal provinces in Canada. Yet during the past decade, New England has reported dramatic decreases in the catch value in this lucrative industry (1). Shell disease is the deterioration of the crustacean exoskeleton by chitinoclastic organisms occurring in both marine and freshwater environments (2). In the past 6 years, the prevalence and severity of shell disease has markedly increased (K. Castro, Rhode Island Sea Grant, pers. comm). Predominately occurring in areas from Buzzard's Bay (Massachusetts) to eastern Long Island Sound (New York), it has been termed epizootic lobster shell disease (ELSD). Recently ELSD lobsters have been observed in Cape Cod Bay (Massachusetts), Kittery (Maine), and in offshore waters of New England (1).

For the present study, carapace lesions from wild-caught specimens of *H. americanus* were examined for the etiological agent responsible for ELSD. Although previous studies on lobster shell disease have used histology and molecular techniques to define the organisms involved in lesions (3, 4) no study has used scanning electron microscopy (SEM) to observe the progression of lesion development. For this study, SEM was used to produce three-dimensional views of ELSD development from geographically distinct areas along the New England coast for site comparisons.

During 2002–2003, lobsters with lesions (n = 22) and without lesions (n = 14) were collected. The sites sampled were the inshore waters of eastern Long Island Sound (n = 4), Rhode Island (n = 13), Buzzards Bay (n = 7), Cape Cod Bay (n = 3), and Maine (n = 4), and the offshore waters of New Hampshire (n = 5). Animals were defined as "healthy" or "infected" depending on the presence of noticeable lesions on the cephalothorax. Carapace pieces were collected, fixed in 10% formalin in sterile seawater (5), and dehydrated in increasing concentrations of ethanol on ice. Samples were trimmed, critical-point-dried, and sputter-coated with gold palladium (6). The surface of cuticle lesions in early disease phases and the deeper interface between lesions and normal cuticle (leading edge of lesions) were compared and analyzed. To compare the presence of morphologically distinct bacteria identified in lesions, images were analyzed using Sigma-Scan 4.0 (Jandel Scientific).

Gross examination of carapace pieces showed that the carapaces of healthy animals showed no degradation, while samples from infected animals were severely eroded. Microscopic analysis of healthy carapace revealed minimal bacterial buildup (Fig. 1A). In contrast, carapace lesions of infected lobsters were covered with bacterial cells. Setal cores and natural abrasions were consistently filled with bacteria embedded in the cuticle at the lesion surface (Fig. 1B). Additionally, bacteria were abundant at the leading edge of the lesions (Fig. 1C). Overall, healthy carapace samples had substantially fewer bacteria on the carapace surface. These observations were consistent for all sampling sites.

The role of bacteria in the progression of lesion development was indicated by bacteria found embedded in shallow pits along the epicuticle (Fig. 1D). In other areas on the surface, halo-like holes surrounded several bacterial types that were associated with shallow erosions. These holes were not observed at the deep leading edges of the lesions. Bore holes appeared to match the length/width ratio of associated bacteria and, therefore, were believed to be caused by bacteria secreting chitinase, lipase, or protease (7). Diatoms, algae, and fungi/actinomycetes were noted typically in low abundance within the cuticle filaments, but bacteria were consistently the dominant organisms on both the carapace surface and the leading edge of lesions.

* Corresponding author: rsmol@mbl.edu

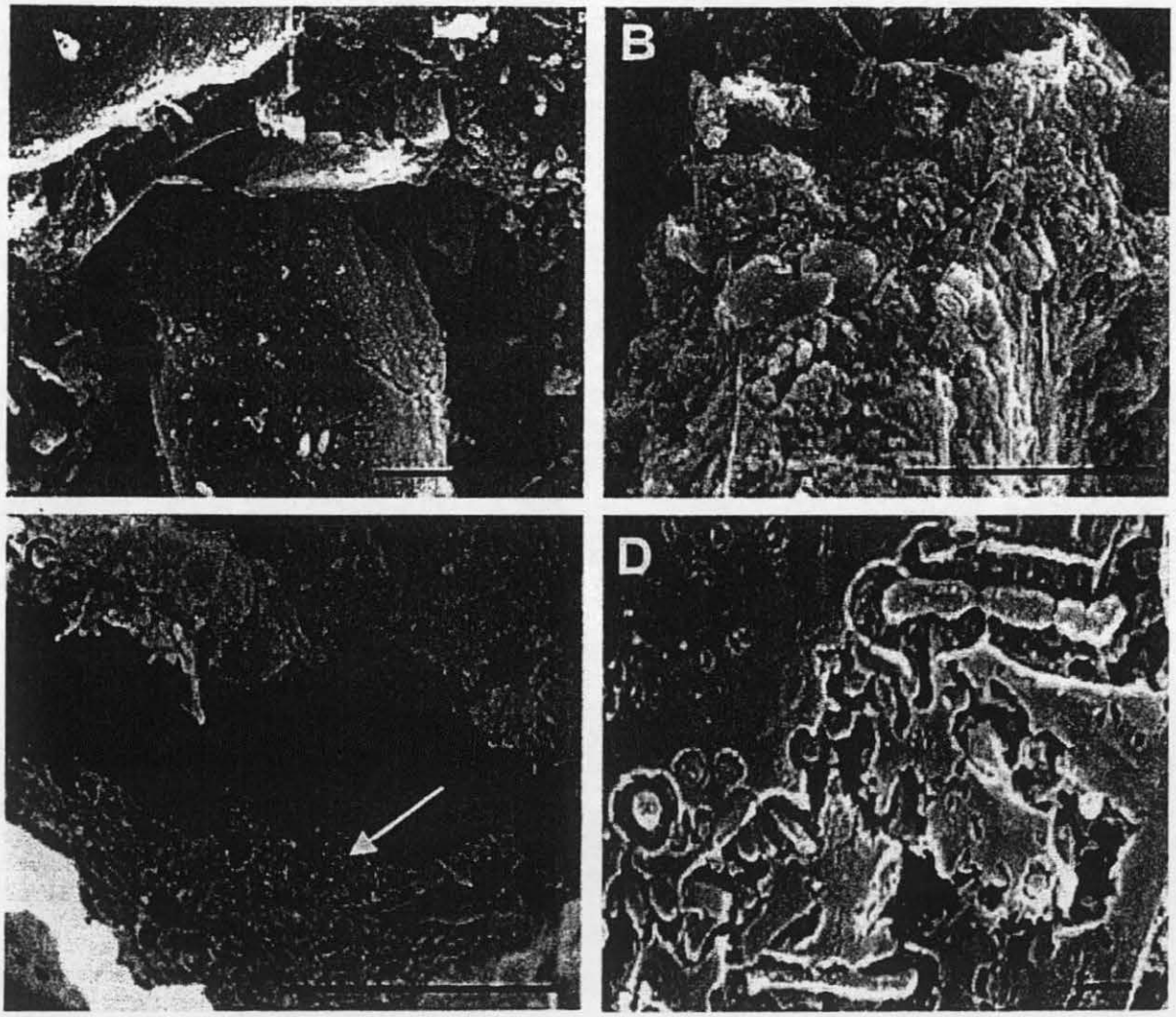

Figure 1. *SEM images from infected and healthy lobsters collected from various sampling sites. (A) Healthy setae with minimal bacterial cells at base of core (arrow) from a non-diseased Maine lobster. (B) Infected setae with a high abundance of bacteria (arrow) from a diseased New Hampshire lobster. (C) Bacterial buildup (arrow) in the leading edge of a lesion from an infected Buzzard's Bay lobster. (D) Enzymatic digest by coccoid, rod, and rod linked bacteria from an infected Buzzard's Bay lobster. Bars represent 10 μm in A, B, and C, and 1 μm in D.*

Five morphologically distinct bacterial types were observed on both healthy and infected animals. The majority of cells were either rods (1 × 0.4 μm), coccoid rods (0.8 × 0.5 μm), or cocci (0.5 × 0.45 μm). Segmented rod links (each piece 1.5 × 0.5 μm) and coccoid links (each piece 1.5 × 1.0 μm) were less abundant and found on infected animals only. Most bacterial types were found on animals from all geographical areas, but coccoid links were observed only on infected Rhode Island and Cape Cod Bay samples, indicating that they may be secondary invaders.

Bacteria are ubiquitous in the marine environment, so identifying the causative agents in a disease can be difficult. Examination of the interface between healthy and necrotic tissue provided the evidence necessary to identify bacteria as the disease-initiating organisms. Scanning electron microscopic imagery cannot speciate bacteria, so additional techniques such as those used in molecular biology are needed to identify the bacteria responsible for ELSD. Findings from the present study revealed the complexity of this disease in its progression and development and demonstrated the necessity for further molecular strides, including bacterial speciation and infection studies, in ELSD research.

Literature Cited

1. **Dean, M. J., K. A. Lundy, and T. B. Hoopes. 2002.** *Massachusetts Division of Marine Fisheries, Technical Report TR-13* (Online). Available: http://www.state.ma.us/dfwele/dmf/index.html [accessed August 2003].
2. **Stewart, J. E. 1980.** Pp. 321–329 in *The Biology and Management of Lobsters,* Vol. 1. J. S. Cobb and B. F. Phillips, eds. Academic Press, New York.
3. **Chistoserdov, A., R. Smolowitz, and A. Hsu. 2003.** Pp. 61–64 in *Connecticut Sea Grant Extension, Third Long Island Sound Lobster Health Symposium.* University of Connecticut, Storrs.

4. **Smolowitz, R. M., R. A. Bullis, and D. A. Abt. 1992.** *Biol. Bull.* **183:** 99–112.
5. **Luna, L. G. 1992.** P. 107 in *Histopathologic Methods and Color Atlas of Special Stains and Tissue Artifacts.* Johnson Printers, Downers Grove, IL.
6. **Flegler, S. L., J. W. Heckman Jr., and K. L. Klomparens. 1993.** Pp. 151–167 in *Scanning and Transmission Electron Microscopy: An Introduction.* Oxford University Press, New York.
7. **Baross, J. A., P. A. Tester, and R. Y. Morita. 1978.** *J. Fish. Res. Board Canada* **35:** 1141–1149.

Reference: *Biol. Bull.* **205:** 230–231. (October 2003)

Characterization of Phosphorus-Regulated Genes in *Trichodesmium* spp.

Elizabeth Orchard[1], Eric Webb[2], and Sonya Dyhrman[2,]*
[1] Cornell University, Ithaca, NY
[2] Woods Hole Oceanographic Institution, Woods Hole, MA

Cyanobacteria of the genus *Trichodesmium* are abundant in tropical and subtropical regions and significantly contribute to carbon and nitrogen fixation in these environments (1). Recent studies suggest that phosphorus (P) supply may influence carbon and nitrogen fixation by *Trichodesmium* in the Atlantic (2, 3). However, evidence of phosphorus deficiency in field populations differs among *Trichodesmium* species (2, 3), suggesting that the individual species may have unique scavenging mechanisms. Here we examine several genes involved in phosphorus physiology within four species, *T. erythraeum, T. tenue, T. thiebautii,* and the related species *Katagnymene spiralis.*

Three genes thought to be related to phosphorus physiology were examined in this study: *phoA* and two copies of *pstS,* designated *pstS1* and *pstS2.* These genes are common components of P-regulated scavenging mechanisms in other cyanobacteria and heterotrophic bacteria (4, 5). The *phoA* gene codes for a predicted alkaline phosphatase, an enzyme that hydrolyzes inorganic phosphorus from organic phosphorus, which can then be used by the organism for growth. The activity of this enzyme has been used as an indicator of phosphorus stress in field populations (2). PstS is a high-affinity binding protein for inorganic phosphorus and is part of a phosphate-induced high-affinity scavenging system.

The sequenced genome of *T. erythraeum* (http://genome.jgi-psf.org/draft_microbes/trier/trier.home.html) was used to identify *phoA* and two copies of *pstS (pstS1* and *pstS2)* on the basis of their similarity to characterized genes in GenBank as part of the ongoing *Trichodesmium* annotation effort (unpubl. data). Multiple primer pairs were designed to amplify internal fragments (referred to as internal) or the complete *phoA, pstS1,* or *pstS2* gene (referred to as external) (Table 1). DNA was extracted following the method described by Orcutt *et al.* (6). PCR amplification conditions were performed with PfuTurbo DNA polymerase (Stratagene, La Jolla, CA) using conditions optimized for each gene and species (Table 1). To optimize amplification, the annealing temperature was varied for each gene and species over a range of at least 25 °C. Other variables included magnesium and enzyme concentration.

We were able to amplify the complete *phoA* and *pstS1* gene from *T. erythraeum* and *T. tenue,* and the complete *pstS2* gene from *T. erythraeum.* We amplified gene fragments from *pstS1* in *T. thiebautii* and *K. spiralis,* and from *pstS2* in *T. tenue* and *K. spiralis* (Table 2). With the entire 3.5 kb of the *phoA* gene amplified from *T. erythraeum,* we were able to clone it into the pBluescript II SK (+) plasmid in *Escherichia coli* DH5α, in order to identify the activity associated with the putative gene. However, activity and expression work is still ongoing.

All PCR products were sequenced at the Josephine Bay Paul Center of the Marine Biological Laboratory (Woods Hole, MA) using the facility's protocols. With the *T. erythraeum* genome as a guide, internal primers were designed to obtain full coverage of the entire gene on both strands. Genes were aligned between species to compare their sequence divergence using Sequencher 4.1 software (Gene Codes Inc. Ann Arbor, MI).

Preliminary sequencing data for the genes and gene fragments indicate that *pstS1, pstS2,* and *phoA* in *T. tenue* as well as *pstS2* in

* Corresponding author: sdyhrman@whoi.edu

Table 1

Primer sequences and annealing temperatures for PCR reactions

Gene	External 5′–3′	Annealing temp.	Internal 5′–3′	Annealing temp.
PhoA	ATGCGTGGGGACTTAACAGTAA	61.2	TTCGCTATCATCATACACCATAATTCCACC	60
	TCTAATCACAAAATCATCTGTTGTGAGAG		AGAACCTAATGATGACTATACTAACGACCC	
PstS1	ACAAGCACAAACTAAAACCAG	58.5	TTTCCATCACCTATATATCAAC	51.2
	GACGAATCAGCAGTGACAAG		CATAACCATACTCAACATATCC	
PstS2	AAATTAGTATCGTTGCCTAAAT	59	ATCTTTTCCAGCTCCACTATAC	50.2
	TTTGTGCTTATACATTTATTATC		CTCCTACTTTCTTTTTCCACTC	